

Some illustrative examples of the use of a spectral-element method in ocean acoustics

Paul Cristini and Dimitri Komatitsch

LMA, CNRS, UPR 7051, Aix-Marseille Univ, Centrale Marseille, F-13402 Marseille Cedex 20, France
cristini@lma.cnrs-mrs.fr, komatitsch@lma.cnrs-mrs.fr

Abstract: Some numerical results in the time domain obtained with the spectral-element method are presented in order to illustrate the high potential of this technique for modeling the propagation of acoustic waves in the ocean in complex configurations. A validation for a simple configuration with a known solution is shown, followed by some simulations of the propagation of acoustic waves over different types of ocean bottoms (fluid, elastic, and porous) to emphasize the wide variety of media that can be considered within the framework of this method. Finally, a movie illustrating upslope propagation over a viscoelastic wedge is presented and discussed.

© 2012 Acoustical Society of America

PACS numbers: 43.20.Gp, 43.30.Ma, 43.58.Ta [JL]

Date Received: December 2, 2011 Date Accepted: January 12, 2012

1. Introduction

The field of numerical modeling of sound propagation in the ocean has been the subject of increasing interest of the underwater acoustics community for many years. Computing an accurate solution, taking a complex environment into account, is still the subject of active research in ocean acoustics for which the objectives are now to focus on simulations in the time domain for 2D configurations with the prospect of being able to handle 3D configurations in the near future. Nowadays, with the stunning increase in computational power, full wave numerical simulation of complex wave propagation problems in the time domain is becoming possible. Several numerical techniques can be used to accurately solve the full wave equation in complex configurations, for instance, the finite-difference method, boundary-element methods, spectral or pseudospectral methods, classical low-order finite-element methods, spectral-element method or discontinuous Galerkin methods. A review of the different numerical techniques commonly used in underwater acoustics can be found in Jensen *et al.*¹ Another technique, the spectral-element method (SEM), which is based upon a high-order piecewise polynomial approximation of the weak formulation of the wave equation, has been the subject of many developments in geophysics in the last 15 yr from the numerical, physical and computational points of view. It was originally developed for Navier Stokes equations² and later adapted to both forward and adjoint/inverse seismological applications^{3,4} and thoroughly validated in that context. It is therefore a good candidate for performing numerical simulations in ocean acoustics in which similar types of media are considered.

The purpose of this letter is to present some illustrative examples that emphasize the high potential of the SEM for underwater acoustic applications. For the sake of simplicity, only two-dimensional configurations will be considered, but a three-dimensional version of the finite spectral-element method already exists and is routinely used, for instance, in geophysics. 2D and 3D versions of an implementation of the SEM, respectively, named SPECSEM2D and SPECSEM3D, are available for free on the Computational Initiative in Geophysics (CIG) website.

In Sec. 2, we will briefly give an introduction to the main characteristics of the SEM and in Sec. 3 we will illustrate its application to ocean acoustics with some

examples including a movie that shows wave propagation following an explosion over a viscoelastic wedge.

2. Short description of the spectral finite element method

Let us briefly recall the main characteristics of the SEM. As pointed out in the Introduction, the spectral-element method is based upon a high-order piecewise polynomial approximation of the weak formulation of the wave equation. It combines the accuracy of the pseudospectral method with the flexibility of the finite-element method. In this method, the wavefield is represented in terms of high-degree Lagrange interpolants, and integrals are computed based upon Gauss–Lobatto–Legendre quadrature. This combination leads to perfectly diagonal mass matrix, which in turns leads to a fully explicit time scheme that lends itself very well to numerical simulations on parallel computers.

It is particularly well suited to handling complex geometries and interface conditions. As a consequence, the accurate simulation of surface wave propagation is straightforward without any additional cost. The use of a pseudospectral method also leads to the generation of coarser meshes. The typical element size that is required to generate an accurate mesh is of the order of λ , λ being the smallest wavelength of waves traveling in the model. This comes from the fact that each spectral element, when using the SEM with a polynomial degree of $N=4$, which is a typical value, contains a subgrid of $(N+1)^2=5 \times 5$ Gauss–Lobatto–Legendre discretization points and requires about 5 points per minimum wavelength of the problem under study. Very distorted mesh elements can be accurately handled.⁵ Complex models that include fluid, elastic, viscoelastic, anisotropic, or porous media⁶ can be modeled, making the SEM a method of choice for the numerical modeling of wave propagation through various types of media encountered in ocean acoustics. Furthermore, the calculation of sensitivity kernels can be performed based on adjoint modeling.^{4,7} Although not considered in this letter, this is a key ingredient for tackling inverse problems. Finally, the SEM is well-suited for parallel implementation on supercomputers, overlapping non-blocking message-passing communications with calculations on the processors to hide their cost;⁸ i.e., performing useful calculations on the processors while communications between processors (based on the Message-Passing Interface library) are traveling across the network connecting them. Clusters of GPU graphics cards can also be used efficiently with the spectral-element method.⁹ This is an important feature for high-performance computing.

3. Underwater acoustics examples

The spectral-element method, because of its ability to handle coupled fluid-solid regions, is a natural candidate for performing wave propagation simulations in underwater acoustics in the time domain. Moreover, it is also known for being accurate to model surface and interface waves.³ In this letter, we thus choose to focus on configurations where such types of waves, also known as Stoneley–Scholte waves, can be generated.

In order to validate the results obtained with this method, let us first consider isovelocity waveguides with flat bottoms, which allow for the comparison with known analytic codes commonly used in underwater acoustics. Since the SEM is a time-domain method, it is necessary to go back to the frequency domain in order to generate the transmission losses. This is performed in two steps. A first step consists in calculating the time series for all receivers. Then, in a second step, a fast Fourier transform is performed for all time sequences to obtain the amplitude of the signal for a given frequency. This way, the transmission losses for any frequency that belongs to the band of the source signal can be calculated. For all the simulations, we consider a Ricker pulse as the source wavelet. We perform the validation of the SEM by making comparisons with the results provided by the SCOOTER FFP code,¹⁰ which we choose because of its robustness and its ability to generate accurate solutions in the near field.

Since the numerical simulations are performed here using the 2D version of the SEM, we use the Cartesian coordinates option available in `SCOOTER` for the generation of the transmission losses. This corresponds to a line source excitation along the third direction (i.e., perpendicular to the 2D plane).

For all the numerical simulations, we take the sound speed in the water layer constant and equal to 1500 m/s and the density of water is equal to 1000 kg/m³.

2.1 Validation for shallow water acoustics

Let us present some results for the validation of the SEM for shallow water propagation simulations. The configuration consists of a waveguide of constant depth 400 m with a point source emitting a Ricker wavelet with a dominant frequency of 30 Hz. The finite element model consists of a structured mesh with a characteristic length about λ . The source depth is 395 m, i.e., close to ocean bottom. The density, compressional and shear wave velocities in the bottom are $\rho = 2000$ kg/m³, $c_p = 2400$ m/s, and $c_s = 1200$ m/s, respectively. With these parameters, a strong interface wave of the Stoneley–Scholte type is excited because the source is close to the interface with the ocean bottom. We consider a horizontal line of receivers situated at depth of 380 m. This array is also located close to the ocean bottom and thus the presence of the interface wave can easily be recorded. The position of the first receiver is $x = 200$ m and that of the last receiver is $x = 4000$ m.

Figure 1 shows a snapshot of the signal received in the horizontal array at $x = 400$ m. The time duration of the generated time sequence is 4.2 s. We do not capture all the successive reflections between the air-water and water-bottom interfaces, but those that are missing have very small amplitudes. Note that the air is not discretized in this study but rather represented by a free surface where pressure is enforced to zero. The first arrival corresponds to the head wave associated to the compressional speed of the ocean bottom, the second arrival is the direct wave that propagates in the water, the third arrival is the Stoneley–Scholte wave whose velocity is $c_{st} = 1005$ m/s and the fourth and strong arrival corresponds to the reflection from the air-water interface.

For all the receivers of the horizontal array, we generate the transmission losses at a given frequency. Figure 2 shows comparisons between the transmissions losses generated from the time sequences calculated with `SPECFEM2D` and those

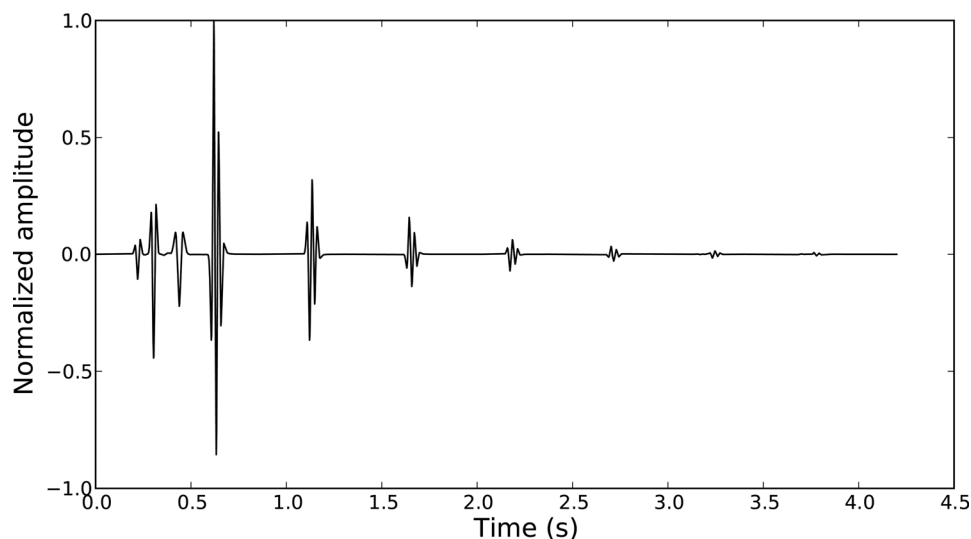


Fig. 1. Snapshot of the pressure signal recorded at position $(x,z) = (400 \text{ m}, 380 \text{ m})$.

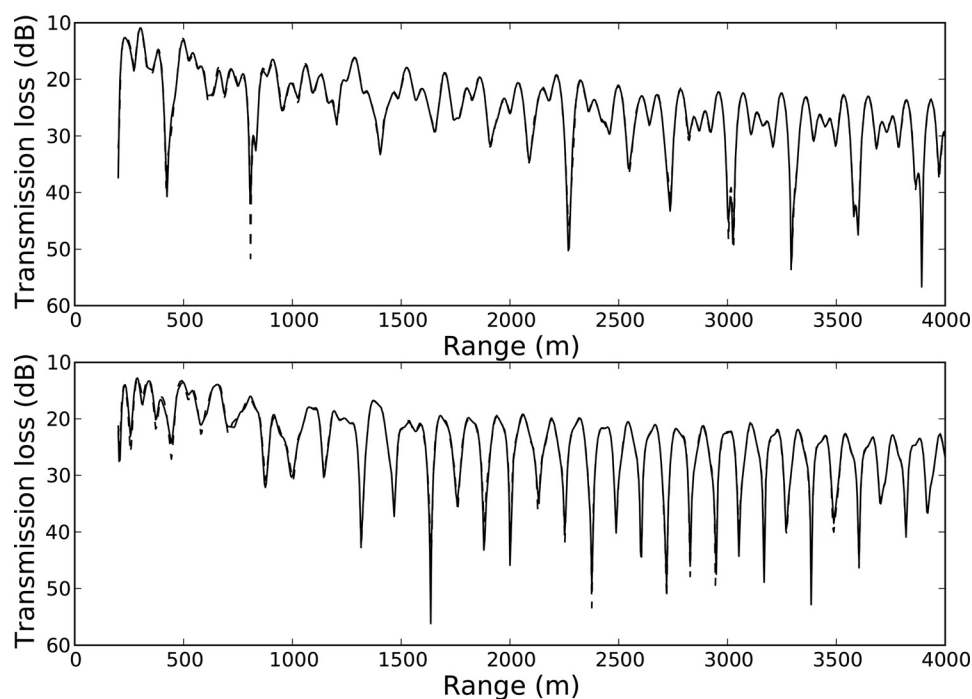


Fig. 2. Transmission loss calculated with SCOOTER (dashed line) and SPECFEM2D (solid line) at 20 Hz (top) and at 30 Hz (bottom).

There is a mistake in the caption here, the figures are for 30 Hz (top) and 40 Hz (bottom).

calculated with SCOOTER. The agreement is almost perfect even if the time duration of the signal is limited.

2.2 Comparisons for different types of ocean bottoms

Since many types of media can be considered with the SEM, let us emphasize the influence of the type of medium that is used as a model of the ocean bottom on the propagation of the acoustic waves in the water column. For this purpose, we first define a porous medium for which we calculate the three different wave velocities that can propagate in such a medium: the fast and slow compressional waves and the shear wave. Then, we define successively an elastic and a fluid medium whose wave speeds are identical to those of the porous medium and have as density the equivalent density of the porous medium. All the physical parameters defining the porous medium are indicated in Table 1. For more information on the type of porous model that is implemented in SPECFEM2D the reader is referred to Morency and Tromp.⁶ We consider a waveguide of constant 400 m depth with a 50 Hz Ricker point source located at a distance of 5 m from the interface with the bottom. The transmission losses calculated for a frequency of 50 Hz are presented in Fig. 3. Two horizontal receiver lines are considered: One close to the interface with the ocean bottom (10 m away from the interface) and one in the middle of the water column. It can be seen that the transmission losses strongly depend on the type of ocean bottom when the receiver line is close to the ocean bottom. The results are very different in the elastic case because of the presence of an interface wave. In the case of a porous bottom, the snapshots indicate the absence of an interface wave, contrary to the elastic case. In future work, the influence of the type of interface conditions between the porous bottom and water will need to be further investigated.

When the receiver line is located in the middle of the water column, the phenomena observed are different. Naturally, there is a difference between a fluid and an

Table 1. Porous medium properties selected for the simulation presented in Fig. 3.

Parameter	Unit	Value
Solid density	kg/m ³	2650
Fluid density	kg/m ³	1000
Porosity	—	0.4
Tortuosity	—	1.25
Solid bulk modulus	GPa	36
Fluid bulk modulus	GPa	2.25
Frame bulk modulus	GPa	2
Fluid viscosity	Pa·s	0
Frame shear modulus	GPa	3.2
Equivalent density	kg/m ³	1990
Fast <i>P</i> speed	m/s	2343
Slow <i>P</i> wave	m/s	1065
<i>S</i> wave	m/s	1385

elastic bottom. The presence of a shear wave strongly modifies the transmission losses but the observed differences between the results with an elastic bottom and with a porous bottom are less pronounced, indicating that the complexity introduced by modeling the ocean bottom with a porous medium does not significantly affect the acoustic wavefield in the middle of the waveguide.

2.3 Propagation over a viscoelastic wedge

The configuration, taken from Ref. 11, corresponds to upslope propagation in a homogeneous water column over a viscoelastic bottom. The compressional and shear wave velocities are 2400 and 1200 m/s, respectively. The density of the ocean bottom is 2000 kg/m³ which corresponds to a chalk-type bottom. Attenuation is modeled in the time domain using two standard linear solids (i.e., damping mechanisms) in order to have a roughly constant attenuation in the frequency band of the emitted signal.³ For both compressional and shear waves, the attenuation is equal to 0.2 dB/λ. The source is situated at the origin of the coordinate system at a depth of 590 m, i.e., close to the ocean bottom. It is a point source emitting a Ricker wavelet with a dominant frequency of 8 Hz. From 0 to 2 km, the waveguide has a constant depth of 600 m. From 2 to 6 km, it decreases linearly to a value of 100 m and then remains constant.

Movie Mm. 1 shows the propagation of the waves generated in this configuration using the SEM. The horizontal size image corresponds to a 14 km long domain. The successive reflections between the air-water and water bottom interfaces can be seen. All these reflections generate successive wavefronts that propagate in the water column and interfere at a certain distance to become one or several modes. The lateral wave that connects by a straight line the two compressional waves that propagate in the water column and in the ocean bottom is also clearly seen. Moreover, an interface wave of the Stoneley–Scholte type is also generated. It can be also noticed, in the first part of the wedge, that there is a stationary regime that is generated and that ends up in backward propagation. This phenomenon may be the cause of the discrepancy between the parabolic equation results and the finite-elements results presented in Fig. 7 of Ref. 11. In that reference this discrepancy occurs at the same place where this phenomenon is present in our movie. Naturally, this requires further investigation to be fully understood but this movie illustrates the amount of information provided by time domain simulations, which can offer new insights into the physics of wave propagation, in particular in complex or coupled media.

Mm. 1. Movie showing acoustic wave propagation in the ocean over a viscoelastic wedge. This is a file of type “animated gif” (12.3 MB).

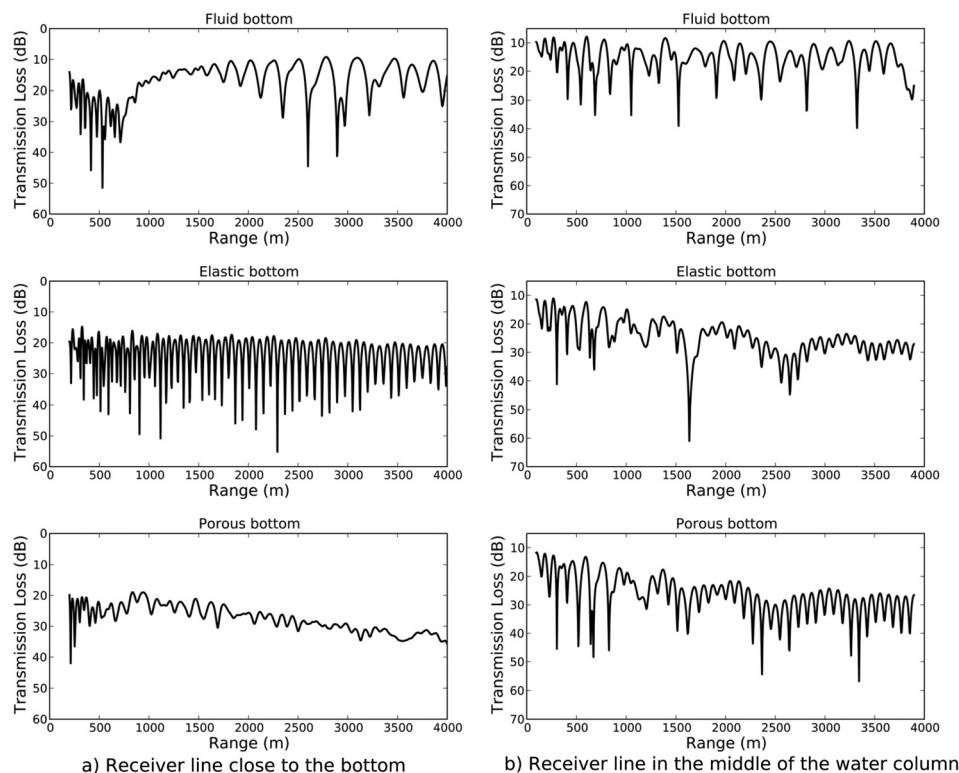


Fig. 3. Transmission losses for different types of ocean bottoms at 50 Hz.

4. Conclusions and future work

We have presented some numerical results obtained with the SEM for ocean acoustic configurations that illustrates the high potential of this method in this domain. The configurations chosen were simple from the geometrical point of view but more complex models can be considered if needed. Rough surfaces as well as buried or immersed objects or sound speed gradients can be modeled because the SEM belongs to the family of finite-element methods. The main difficulty lies in meshing the model. This difficulty can be overcome with modern meshing software packages. Moreover, for some situations in which the size of the problem is small, many simulations can be performed with different rough surface realizations, which makes it possible to tackle reverberation problems. A large variety of problems can be handled, which makes the SEM a method of choice for the numerical simulation of full wave propagation in ocean acoustics.

In future work we will report results for more complex models. For instance, we think that the numerical simulation of the 2D full wave propagation in the time domain of a few kHz source signal in a few kilometers long domain is possible on a modern computing cluster with a few hundred processor cores. If the source frequency is lowered, the size of the domain can be increased and vice versa. 3D simulations are also possible but may require a larger computer.

References and links

- ¹F. Jensen, W. Kuperman, M. Porter, and H. Schmidt, *Computational Ocean Acoustics*, 2nd ed. (Springer, Berlin, 2011).
- ²A. T. Patera, "A spectral element method for fluid dynamics: laminar flow in a channel expansion," *J. Comp. Phys.* **54**, 468–488 (1984).

- ³D. Komatitsch and J. Tromp, "Introduction to the spectral-element method for 3-D seismic wave propagation," *Geophys. J. Int.* **139**, 806–822 (1999).
- ⁴J. Tromp, D. Komatitsch, and Q. Liu, "Spectral-element and adjoint methods in seismology," *Commun. Comput. Phys.* **3**, 1–32 (2008).
- ⁵S. P. Oliveira and G. Seriani, "Effect of element distortion on the numerical dispersion of spectral element methods," *Commun. Comput. Phys.* **9**, 937–958 (2011).
- ⁶C. Morency and J. Tromp, "Spectral-element simulations of wave propagation in poroelastic media," *Geophys. J. Int.* **175**, 301–345 (2008).
- ⁷D. Peter, D. Komatitsch, Y. Luo, R. Martin, N. Le Goff, E. Casarotti, P. Le Loher, F. Magnoni, Q. Liu, C. Blitz, T. Nissen-Meyer, P. Basini, and J. Tromp, "Forward and adjoint simulations of seismic wave propagation on fully unstructured hexahedral meshes," *Geophys. J. Int.* **186**, 721–739 (2011).
- ⁸S. Tsuboi, D. Komatitsch, C. Ji, and J. Tromp, "Spectral-element simulations of the November 3, 2002, Denali, Alaska earthquake on the Earth Simulator," *Phys. Earth Planet. Inter.* **139**, 305–313 (2003).
- ⁹D. Komatitsch, "Fluid-solid coupling on a cluster of GPU graphics cards for seismic wave propagation," *C. R. Acad. Sci., Ser. IIb Mec.* **339**, 125–135 (2011).
- ¹⁰M. B. Porter, "The KRAKEN normal mode program," SACLANTCEN memorandum SM-245, La Spezia, Italy (1991).
- ¹¹F. B. Jensen, P. L. Nielsen, M. Zampolli, M. D. Collins, and W. L. Siegmund, "Benchmark scenarios for range-dependent seismo-acoustic models," in *Theoretical and Computational Acoustics 2007*, edited by M. Taroudakis and P. Papadakis (E-MEDIA University of Crete, Heraklion, Crete, Greece, 2008).